STEM CELLS AND DEVELOPMENT
Volume 31, Numbers 19–20, 2022

DOI: 10.1089/scd.2022.0003

Limited Efficacy of Adipose Stromal Cell Secretome-Loaded Skin-Derived Hydrogels to Augment Skin Flap Regeneration in Rats

Linda Vriend,[1,2] Joris A. van Dongen,[2,3] Viktor Sinkunas,[4] Linda A. Brouwer,[1] Henk J. Buikema,[1] Luiz F. Moreira,[4] Rolf Gemperli,[5] Laura Bongiovanni,[6,7] Alain de Bruin,[6,7] Berend van der Lei,[2] Cristina P. Camargo,[5] and Martin C. Harmsen[1]

Insufficient vascularization is a recurring cause of impaired pedicled skin flap healing. The administration of adipose tissue-derived stromal cells' (ASCs') secretome is a novel approach to augment vascularization. Yet, the secretome comprised of soluble factors that require a sustained-release vehicle to increase residence time. We hypothesized that administration of a hydrogel derived from decellularized extracellular matrix (ECM) of porcine skin with bound trophic factors from ASCs enhances skin flap viability and wound repair in a rat model. Porcine skin was decellularized and pepsin-digested to form a hydrogel at 37°C. Conditioned medium (CMe) of human ASC was collected, concentrated 20-fold, and mixed with the hydrogel. Sixty Wistar rats were included. A dorsal skin flap (caudal based) of 3×10 cm was elevated for topical application of DMEM (group I), a prehydrogel with or without ASC CMe (groups II and III), or ASC CMe (group IV). After 7, 14, and 28 days, perfusion was measured, and skin flaps were harvested for wound healing assessment and immunohistochemical analysis. Decellularized skin ECM hydrogel contained negligible amounts of DNA (11.6 ± 0.6 ng/mg), was noncytotoxic and well tolerated by rats. Irrespective of ASC secretome, ECM hydrogel application resulted macroscopically and microscopically in similar dermal wound healing in terms of proliferation, immune response, and matrix remodeling as the control group. However, ASC CMe alone increased vessel density after 7 days. Porcine skin-derived ECM hydrogels loaded with ASC secretome are noncytotoxic but demand optimization to significantly augment wound healing of skin flaps.

Keywords: ASC, wound healing, ECM, skin flap, ASC secretome, hydrogels, adipose-derived stromal cells

Introduction

Pedicled skin flaps are a Gold standard to repair tissue defects in reconstructive surgery. The survival of these flaps primarily depends on maintenance or restoration of adequate perfusion at the pedicle base [1]. Obviously without appropriate perfusion, severe ischemia occurs that impairs skin flap healing, which occurs infrequently. Tissue ischemia causes vasoconstriction, which further decreases flap perfusion, leading to wound dehiscence and subsequent loss of tissue due to necrosis. Subsequently, patients suffering from local necrosis-induced tissue loss are prone to infection and sepsis. These complications require additional surgery to cover the defect. This causes prolonged hospitalization and increased health care costs.

Improving skin flap survival has focused mainly on stimulating angiogenesis and perfusion by topical application of pharmaceutical agents, for example, sildenafil, minoxidil, nifedipine, and nitroglycerin [2–5]. These pharmaceutical

Departments of [1]Pathology & Medical Biology and [2]Plastic Surgery, University Medical Center Groningen, University of Groningen, Groningen, the Netherlands.
[3]Department of Plastic Surgery, University Medical Center Utrecht, University of Utrecht, Utrecht, the Netherlands.
[4]Department of Cardiovascular Surgery, Universidade of Sao Paulo, Sao Paulo, Brazil.
[5]Department of Plastic Surgery Microsurgery and Plastic Surgery Laboratory, Universidade of Sao Paulo, Sao Paulo, Brazil.
[6]Department of Pediatrics, University Medical Center Groningen, University of Groningen, Groningen, the Netherlands.
[7]Department of Biomolecular Health Sciences, Faculty of Veterinary Medicine, Utrecht University, Utrecht, the Netherlands.

agents temporarily improve flap viability. Yet, they do not always induce neoangiogenesis, and repeated administration is necessary to prolong increased perfusion, which comes with undesirable systemic side effects, for example, peripheral vasodilatation. Thus, currently no ideal treatment exists that adequately improves vascularization of poor vascularized pedicled skin flaps to prevent flap failure.

In recent years, adipose tissue-derived content and more specifically adipose tissue-derived stromal cells (ASCs) have proven an excellent source for regenerative therapies, including wound healing. Their angiogenesis inducing properties and secreted proregenerative trophic factors or secretome (ASC CMe) have provided a new treatment modality to augment skin flap viability [6–10]. ASCs are multipotent progenitor cells [11–17] that remodel extracellular matrix (ECM) through secretion of matrix metalloproteinases and deposition of ECM components, and can inhibit apoptosis, modulate the immune response, promote angiogenesis and parenchymal proliferation through joint secretion of soluble factors such as growth factors, cytokines, and chemokines.

ASCs' paracrine factors alone enhance skin flap healing and direct tissue regeneration in skin flaps [18–21]. However, rapid diffusion of the low molecular weight trophic factors limited their therapeutic capability. The use of a delivery vehicle that binds these trophic factors, in particular growth factors, and release of these trophic factors in a sustained manner are therefore indicated.

Recently, we showed with in vitro studies that ECM hydrogels of cardiac and adipose origin act as a slow-release platform for bound ASC-secreted growth factors, and enhance endothelial cell proliferation [22]. Moreover, ECM regulates vital cellular functions, for example, survival, differentiation, growth, and migration [23,24] by transducing biochemical cues to surrounding cells that may subsequently augment tissue repair.

Hence, the use of this novel sustained-release vehicle consisting of ECM hydrogels loaded with ASC CMe might increase angiogenesis and thereby improve vascularization of pedicled skin flaps. In this study, ECM hydrogels derived from decellularized porcine skin loaded with ASC CMe are deployed to improve vascularization of pedicled skin flaps in a rat model.

Materials and Methods

Decellularization of porcine skin

Skin of 10–12 weeks old pigs was decellularized using a similar recently published protocol [25–27]. In brief, excessive subcutaneous tissue was excised, and remaining skin tissue was blended until a homogeneous paste had formed. The tissue paste was centrifuged at 3,000 *g* for 3 min with phosphate-buffer saline (PBS) and subsequently sonicated at room temperature (RT) for 1 min. The suspension was treated with 0.05% Trypsin/PBS and shaken constantly at 37°C for 4 h.

After washing overnight, tissue was incubated with 1% sodium dodecyl sulfate (SDS; Sigma-Aldrich, St. Louis, MO), followed by 1% Triton X-100 (Sigma-Aldrich) and finally with 1% deoxycholate (Sigma-Aldrich), all under constant stirring at 37°C for 24 h. Finally, decellularized matrix (dECM) was treated with DNase (LS002007, Worthington, final concentration of 30 μg/mL DNAse in 1.3 mM $MgSO_4$ and 2 mM $CaCl_2$) under constant stirring at 37°C for 24 h. dECM was stored in 70% ethanol at 4°C before experimental use.

Characterization of decellularized porcine skin

Pulverized native porcine skin and dECM of porcine skin were formalin-fixed and embedded in paraffin [25]. Five micrometer sections were mounted on glass microscope slides, and deparaffinized for staining with hematoxylin and eosin (H&E) and Movat's pentachrome. After staining, slides were mounted and visualized under a light microscope (Leica Microsystems, DM IL).

Nuclear content measurement

Decellularized porcine skin was assessed for genomic DNA presence. Ten milligram dECM was dissolved in 5 μL proteinase K (2 U/mg, Sigma-Aldrich; 3115828001), 50 μL 10% SDS and 500 μL SE-buffer (75 mM NaCl, 25 mM EDTA; pH 8.0), and incubated at 55°C overnight. Subsequently, 6 M NaCl and chloroform were added to the solution, shaken extensively in a top-over-top rotator for 45 min at RT, and centrifuged at 2,500 *g* at 20°C for 10 min.

The upper layer was pipetted and gently mixed with ice-cold isopropanol, and centrifuged at 13,000 *g* at 4°C for 15 min. The remaining pellet was washed with 70% ethanol and centrifuged again at 10,000 *g* at 4°C for 5 min. Next, TE (10 mM Tris, 0.1 mM EDTA; pH 8.0) was added to the pellet, and DNA was quantified using NanoDrop equipment (Thermo Scientific, Hemel Hempstead, United Kingdom). In addition, a 4′,6-diamidino-2-phenylindole (DAPI, 4 μg/mL; #D9542-5MG, blue; Sigma-Aldrich) staining was performed to assess the presence of residual nuclei and visualized under a fluorescence microscope (Leica Microsystems, DM IL).

Isolation of human ASCs & collection and characterization of conditioned medium

Human ASCs were isolated and characterized as described previously [26]. In brief, human adipose tissue was obtained from healthy donors ($n = 3$) during regular liposuction procedures. Lipoaspirate was digested enzymatically with 0.1% Collagenase A (#11088793001; Roche Diagnostic, Mannheim, Germany) in PBS with 1% bovine serum albumin (BSA, #A9647; Sigma-Aldrich, Boston, MA) and shaken constantly at 37°C for 1.5 h. Digested tissue was placed in lysis buffer on ice to disrupt erythrocytes. Cells were then centrifuged and cultured at 37°C at 5% CO_2 in humidified incubator in Dulbecco's modified Eagle's medium (DMEM; BioWhittaker Walkersville, MD: 10% fetal bovine serum (FBS), 1% L-Glutamine (L-Glut) [Lonza (BE17-605E), 1% Penicillin/Streptomycin (P/S)] (10,000 U/mL, Invitrogen; 15140-122).

Medium was changed twice a week. Cells were characterized based on CD marker surface expression using flow cytometry (CD29, CD31, CD44, CD45, CD90, and CD105), adipogenic, osteogenic, and smooth muscle cell differentiation capacity as well as colony formation capacity. After confirmation, remaining FBS was washed out extensively with PBS. ASC CMe was then obtained from confluent

cultures of ASCs in blank medium (FBS deprived) between passages 3 and 6. ASC CMe was collected after 24 h and filtered through a 0.22 µm filter (Corning; 431229). Then, ASC CMe was concentrated using 3 kDa cutoff Amicon Ultra Centrifugal filters (Sigma-Aldrich).

Preparation of ECM hydrogels incubated with ASC-derived conditioned medium

The manufacturing of ECM-based hydrogels was performed as reported previously [25–27]. In brief, 40 mg of dECM tissue was digested in a solution of 2 mg/mL porcine pepsin (3,200 I.U.; Sigma-Aldrich) in 0.01 M hydrochloric acid (HCl) and stirred constantly at 500 rpm at RT for 6 h. The resulting pregel solution was neutralized (pH 7.4) with 0.1 M sodium hydroxide, followed by adding 1/18 volume of ASC CMe. Growth factors present in ASC CMe were allowed to bind to ECM at 4°C for 24 h.

Subsequently, the addition of 1/18 volume of 20-×PBS led to a final concentration of 1×PBS pregel solution. A single bare dECM hydrogel was preserved for histological examination. The hydrogel was formalin-fixed, embedded in paraffin, and sectioned at five micrometer thickness. Sections were deparaffinized for H&E staining, dehydrated and mounted in xylene-based medium, and visualized by microscope.

Skin flap in vivo experiment

The experiment was performed with approval from the Ethical Committee of the University of São Paulo, Brazil (1197/2018). The study followed ethical principles for animal research according to the National Council of Animal Experimentation (NCAE/2013). Sixty 8-week-old male Wistar rats (weight 250–300 g) were used in this pedicled skin flap model. All rats were anesthetized by intraperitoneal injection of a mixture of 100 mg/kg ketamine hydrochloride (Ketamin®; Cristália, Brasil) and 5 mg/kg xylazine hydrochloride (Rompun®; Bayer, Brazil). Then, rats were positioned in ventral decubitus followed by epilation of the hair on the dorsal region.

Aqueous 0.5% chlorhexidine was used for antisepsis of the surgical field. Next, the modified skin as described by Camargo et al. was designed at the rats' back [28]. The flap was sharply dissected in the areolar tissue plane, deep to the level of the panniculus carnosus and up to the interscapular base. Next, the flap was elevated. Then, the animals were divided into four groups ($n=5$): DMEM (group I), ECM hydrogel (group II), ECM hydrogel with CMe (group III), and CMe (group IV). After topical application, the flap was sutured into place with 4-0 monofilament nylon single stitches at 0.5 cm intervals. All rats were housed in separate cages after surgery to prevent flap cannibalism. Food and water were offered ad libitum in a 25°C environment and in a controlled day and night cycle (12 h light/12 h dark).

Rats were observed daily and received humane care according to regulations on animal experiments of the Council for International Organization of Medical Sciences (CIOMS). Rats were harvested at 7, 14, and 28 days using an intraperitoneal injection of 200 mg/kg ketamine hydrochloride and 15 mg/kg xylazine hydrochloride. The entire flap was sharply dissected and trichotomized in a proximal, medial, and distal part and harvested for histological examination (Supplementary Fig. S1).

Macroscopic wound healing index

Photographs of skin flaps were taken with a digital camera before treatment and directly after euthanizing at 7, 14, and 28 days under identical conditions. Distal, medial, and proximal wound surface areas were scored double blinded and randomized (computer assisted) by independent observers on a score from 0 to 6 (Fig. 1A and Supplementary Fig. S2). Macroscopic scoring was based on clinical experience; a low score corresponded with near to healing, a high score to necrotic, unhealed tissue. An interobserver reliability test was performed by linear regression to assess reliability. In addition, wound surface area was calculated as a percentage of the total skin flap. Total pixels per area were measured using the measurement tool in Fiji ImageJ (ImageJ; National Institutes of Health, Bethesda, MD), and wound surface percentage was calculated.

Blood flow by Doppler analysis

Laser Doppler perfusion imaging analysis (PowerLab 4/26 LabChart Pro, USA Flowmeter) was performed to measure perfusion in the distal, medial, and proximal area of the skin flap before creating the flap, directly after the flap was sutured back into place and before sacrifice at 7, 14, and 28 days. Measurements were performed with a pinpoint probe. Correlation between wound surface area and perfusion was analyzed.

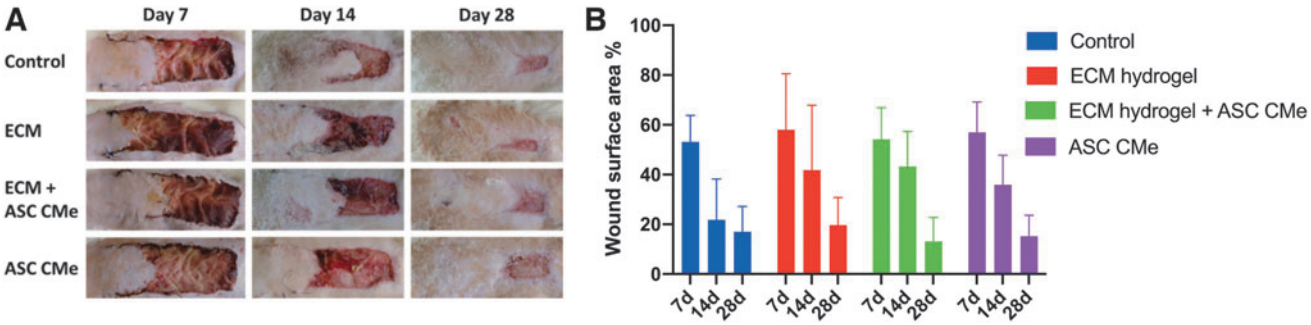

FIG. 1. **(A)** Standardized photographs of skin flap wound healing on days 7, 14, and 28 in rats ($n=5$) treated with DMEM (control), ECM hydrogel, ECM hydrogel + ASC CMe, and ASC CMe. **(B)** Wound surface area in skin flaps decreased over time, no significant differences were observed between groups (n = 5). DMEM, Dulbecco's modified Eagle's medium; ECM, extracellular matrix; ASC, adipose tissue-derived stromal cell; CMe, conditioned medium.

Histological wound analysis

Skin flap wound tissue sections were formalin-fixed, embedded in paraffin, and sectioned at four micrometer thickness. Sections were deparaffinized and stained with H&E, Picrosirius, Masson's Trichrome. For collagen analysis, micrographs were taken from picrosirius staining with the fluorescent microscope, and analysis of collagen width, length, and angle was performed with CT-FIRE V2.0 Beta (https://eliceirilab.org/software/ctfire/).

Qualitative and quantitative assessment of angiogenesis

A board-certified veterinary pathologist (blinded to group allocation) independently performed qualitative assessment of angiogenesis on H&E-stained sections of the distal, medial, and proximal area of the skin flap after 7 and 14 days ($n=3$ per area and per group). A four-point scale was used reflecting (1), scattered (2) a few (3) moderate number and (4) numerous amount of blood vessels on three levels: (1) dermis, (2) hypodermis/muscle, and (3) deep fascia.

An additional quantitative analysis was performed by two independent observers (blinded samples) on the same sections at 7 days follow-up ($n=3$ per area and per group). Each observer counted arterioles in 10 random fields per section at 20× magnification. Sections with large differences in the count of arterioles were recounted by the senior observer. An inter-rater coefficient was calculated.

Immunohistochemical wound analysis

Fixed wound tissue sections were deparaffinized and treated with 10 mM Tris-Cl (pH 7) at 85°C overnight. After serum blocking, slides were incubated with primary antibody rabbit anti-Ki67 (#ab16667, Abcam; 1:200) or mouse antirat CD68 (#MCA 341R; Bio-Rad, Veenendaal, Netherlands 1:120 or 1:166) for both at RT for 1 h. Endogenous peroxidase was blocked with 0.1% H_2O_2, for Ki-67 also endogenous biotin blocking was performed with biotin blocking system (#X0590; DAKO).

As secondary antibodies goat antirabbit-biotin (#E0432, DAKO; 1:100) for Ki-67 and rabbit antimouse-HRP (#P0260, DAKO; 1:100) for CD68 were used. Thereafter, Ki-67–stained tissues were incubated with streptavidin-HRP (#P397, DAKO; 1:200). AEC was used to develop color, and counterstaining was performed with hematoxylin. The fraction of Ki-67- and CD68-positive cells was determined using VisioPharm software (Visiopharm, Cophenhagen, Denmark).

Statistical analysis

All experimental data represent the mean of three or five independent experiments performed in duplicate per treatment and per follow-up moment. Results are presented as mean with standard error of the mean and analyzed using Graphpad Prism (version 8.4; GraphPad Software, Inc., La Jolla, CA). Test for normality was performed with D'agostino-Pearson. One-way analysis of variance (ANOVA) with Tukey's multiple comparison post hoc test was carried out for more than three test groups. Two-way ANOVA Dunnet's multiple comparison test was used to calculate differences between all groups. P values <0.05 were considered statistically significant. The nonparametric variables were tested by the Kruskal–Wallis test. For post hoc comparisons, Dunn's test was applied.

Results

Decellularization of porcine skin results in acellular matrix and is devoid of nuclear remnants

The dECM comprised a fibrous structure with minimal residual cellular remnants as shown by H&E staining (Supplementary Fig. S3A, B). dECM contained negligible amounts of DNA (11.6 ± 0.6 ng/mg, $n=3$), which is in accordance with the advised maximum value for decellularized tissue [29].

Wound healing index

All wound surface areas reduced over time and resulted in completely healed skin (Fig. 1A). After 7 days, the remaining wound surface areas were similar, irrespective of treatment, and ranged between 53% and 58%. After 14 days, all groups showed similar surface areas (range from 36% to 43%) compared with the DMEM group (22%). After 28 days, wound surface areas ranged from 13% to 20% (Fig. 1B). Complications such as infection and wound dehiscence did not occur.

The wound healing index (WHI) in the distal area increased in the experimental and ECM hydrogel group after 14 days, compared with the DMEM group ($P<0.05$, Fig. 2A). This effect was nullified after 28 days. In the medial area, WHI increased in the ECM hydrogel and CMe group compared with the DMEM group ($P<0.01$, Fig. 2B), and WHI increased in the ECM hydrogel with CMe group compared with the DMEM group ($P<0.001$) after 14 days. In the proximal area, WHIs between groups were comparable at all follow-up moments (Fig. 2C). Irrespective of treatment, the proximal and distal area showed a difference; WHI in the distal area ranged between 2 and 5, and in the proximal area it ranged between 0 and 2. The interobserver reliability test showed to be negligible (Supplementary Fig. S4).

Wound perfusion

Blood perfusion in the distal area was absent in all groups after 7 days (Fig. 3A), which was restored after 14 days. In the medial area, lower perfusion was measured in the ECM hydrogel with CMe, ECM hydrogel, and the CMe group compared with the DMEM group after 7 days (Fig. 3B). Perfusion in the proximal area remained constant from days 7 to 28 (Fig. 3C). The restored perfusion was eventually higher in the distal and medial area than in the proximal area. Furthermore, correlation between wound surface area and blood flow was analyzed regardless of intervention group (Fig. 4). High wound surface area was correlated with low perfusion after 7 days ($P<0.01$).

Qualitative assessment of angiogenesis score demonstrated minimal differences between groups after 7 and 14 days (Fig. 5A, B). Quantitative analysis showed an increased vessel density in ASC CMe versus DMEM ($P<0.0001$), ECM hydrogel ($P<0.0001$), and ECM hydrogel with CMe ($P<0.0001$) in the distal area after 7 days ($n=3$) (Fig. 5C). The inter-rater coefficient was 60%.

Cellular assessments

Of all cells, 1% to 6% cells were proliferating in the skin flap, as shown by Ki-67 staining (Fig. 6). In the distal, medial, and

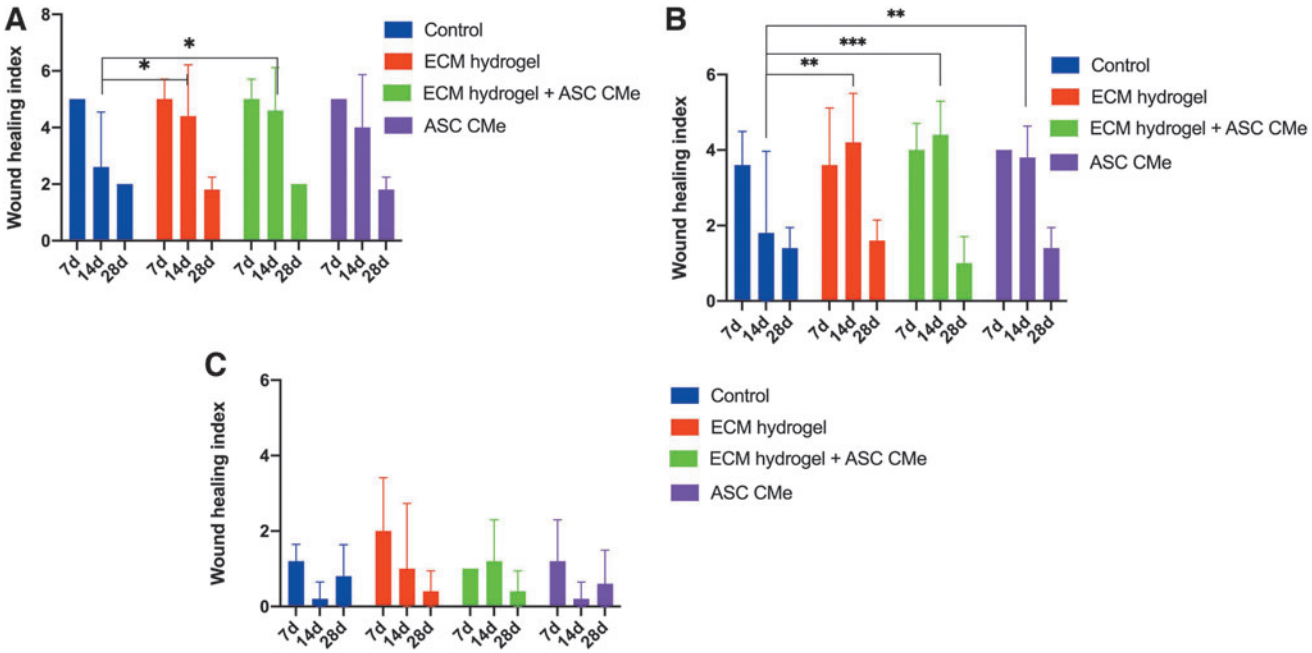

FIG. 2. Wound healing index in control, ECM hydrogel, ECM hydrogel + ASC-CMe, and ASC-CMe group after 7, 14, and 28 days ($n=5$) in distal **(A)**, medial **(B)**, and proximal **(C)** wound area. Lower wound healing index corresponds with better wound healing. **(A)** Wound healing index in control group is lower than that in ECM hydrogel and ECM hydrogel +ASC-CMe groups after 14 days ($P<0.05$*). **(B)** Wound healing index in control group is lower than that in ECM hydrogel and ASC-CMe group ($P<0.01$**) and lower than ECM hydrogel +ASC-CMe ($P<0.001$***) after 14 days.

proximal area, the number of proliferating cells was similar between groups. Clustering of macrophages was apparent between dermis and the epidermal layer, close to the wound crust, indicating cells are clearing wound debris. In distal and medial areas, the presence of macrophages was similar, irrespective of treatment after 7, 14, and 28 days (Fig. 7). In the proximal area, CMe group had a lower influx of macrophages compared with the DMEM group after 14 days ($P<0.05$).

Matrix remodeling

Width, length, and angle of collagen fibers were comparable between groups in the distal, medial, and proximal area at all follow-up moments (Fig. 8). As exception, only width in the ECM hydrogel group decreased significantly compared with the DMEM group after 7 days in the proximal area.

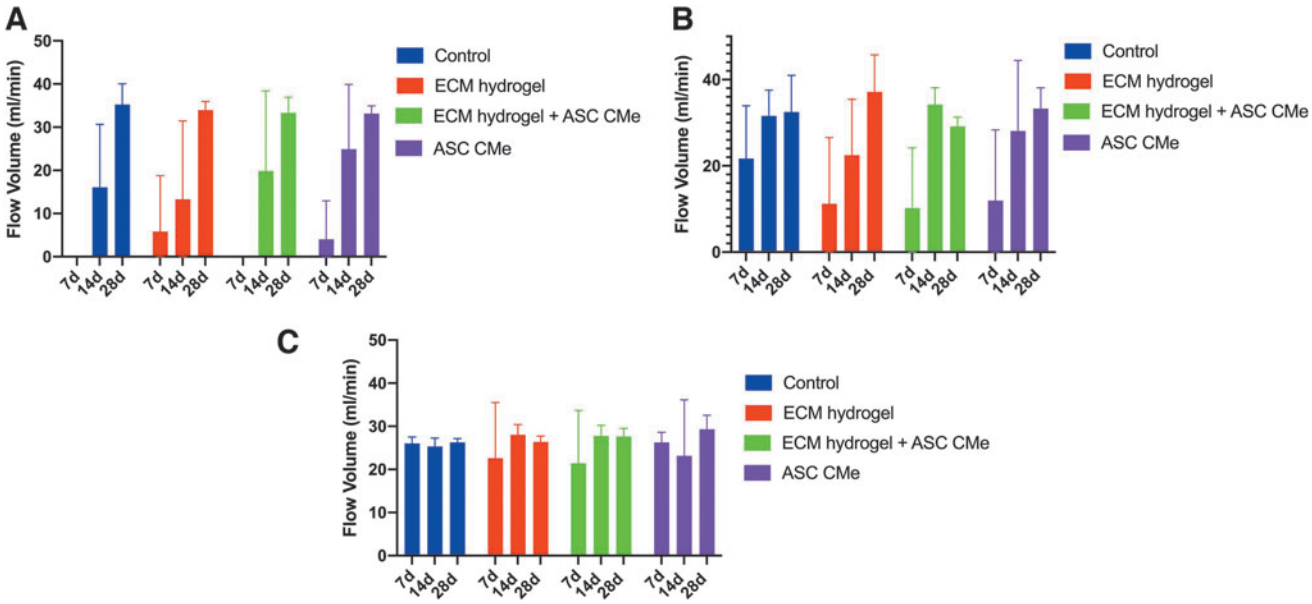

FIG. 3. Skin flap blood flow (mL/min) in distal **(A)**, medial **(B),** and proximal **(C)** area measured with laser doppler in control, ECM hydrogel, ECM hydrogel + ASC-CMe, and ASC-CMe group after 7, 14, and 28 days ($n=5$).

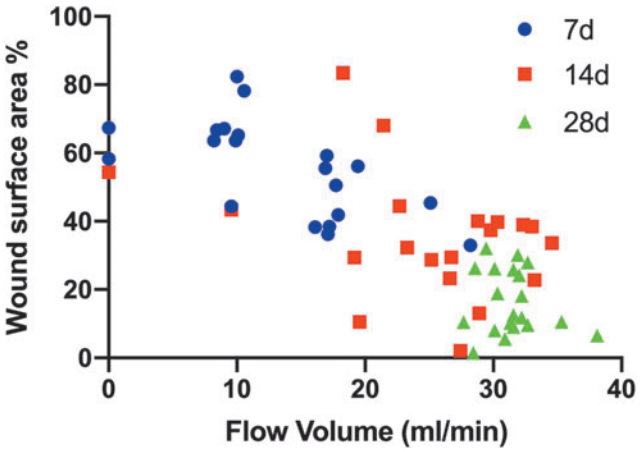

FIG. 4. Wound surface area versus laser doppler after 7, 14, and 28 days. Correlation of necrosis versus doppler signal (flow volume (mL/min)) ($n = 20$) after treatment for 7, 14, and 28 days regardless of treatment. Significant negative correlation after 7 days treatment ($P < 0.01$**).

Discussion

This study unexpectedly demonstrated that ECM hydrogels loaded with ASC secretome did not influence dermal wound healing in a pedicled skin flap rat model as compared with the control groups microscopically, macroscopically, and functionally. However, this study did demonstrate that ASC secretome enhanced angiogenesis in ischemic parts of the skin flap.

Currently available pharmaceutical agents do not suffice to augment flap viability in clinical setting. Therefore, this study was undertaken to investigate the possible efficacy of ASC secretome-loaded ECM hydrogels in a skin flap rat model. To the best of our knowledge, this is the first study of its kind that also comprehensively assessed several relevant wound healing processes; that is, angiogenesis, cell proliferation, immune modulation, and matrix remodeling.

In search for an off-the-shelf product with strong regenerative capability, we aimed to synergistically combine organ-derived ECM and ASCs' secretome in a hydrogel. ASC secretome namely comprises all growth factors to direct tissue healing and can be retained in a delivery vehicle, that is, ECM. In this study, an efficient, reproducible decellularization procedure yielded porcine skin ECM, which was successfully formulated into a hydrogel with bound ASC secretome that complies with current guidelines [29]; that is, it comprised of minimal DNA content and no cellular remainders.

After both ECM hydrogel treatments, the observed macroscopic wound healing and low immune cell influx were similar to control groups. This indicates that ECM hydrogels are well tolerated, noncytotoxic, and do not inflict a host immune response in rats. ASC secretome treatment did

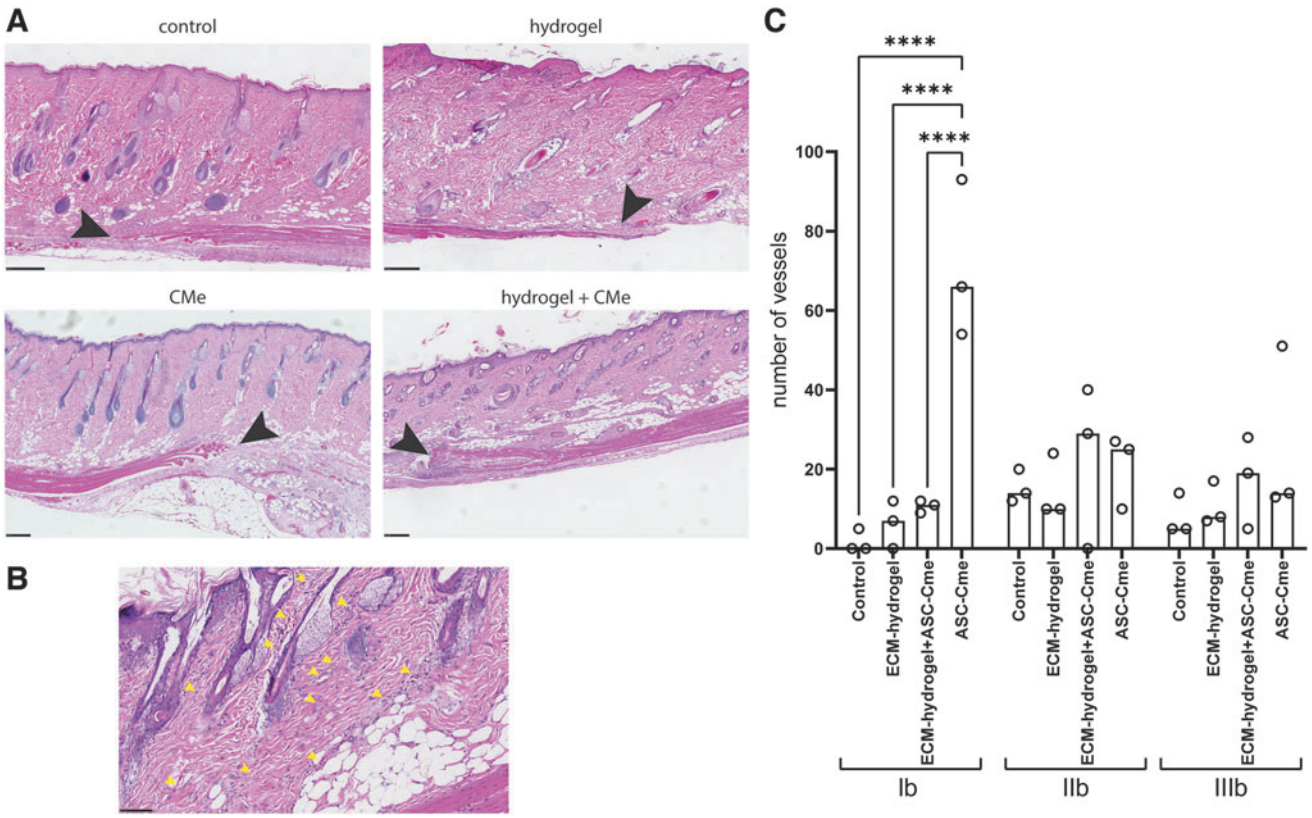

FIG. 5. **(A, B)** Microscopic H&E-stained images of control and ECM hydrogel, ECM hydrogel + ASC-CMe, and ASC-CMe group of medial area after day 7. **(C)** Angiogenesis index in the distal, medial, and proximal area based on number of vessels in control, ECM hydrogel, ECM hydrogel + ASC-CMe, and ASC-CMe group after 7 days ($n = 3$). Black arrows indicate where treatment was injected. Yellow arrows show newly formed capillaries. Significantly higher amount of vessels in the ASC-CMe group compared to control, ECM hydrogel and ECM hydrogel + ASC-CMe group ($P < 0.0001$****).

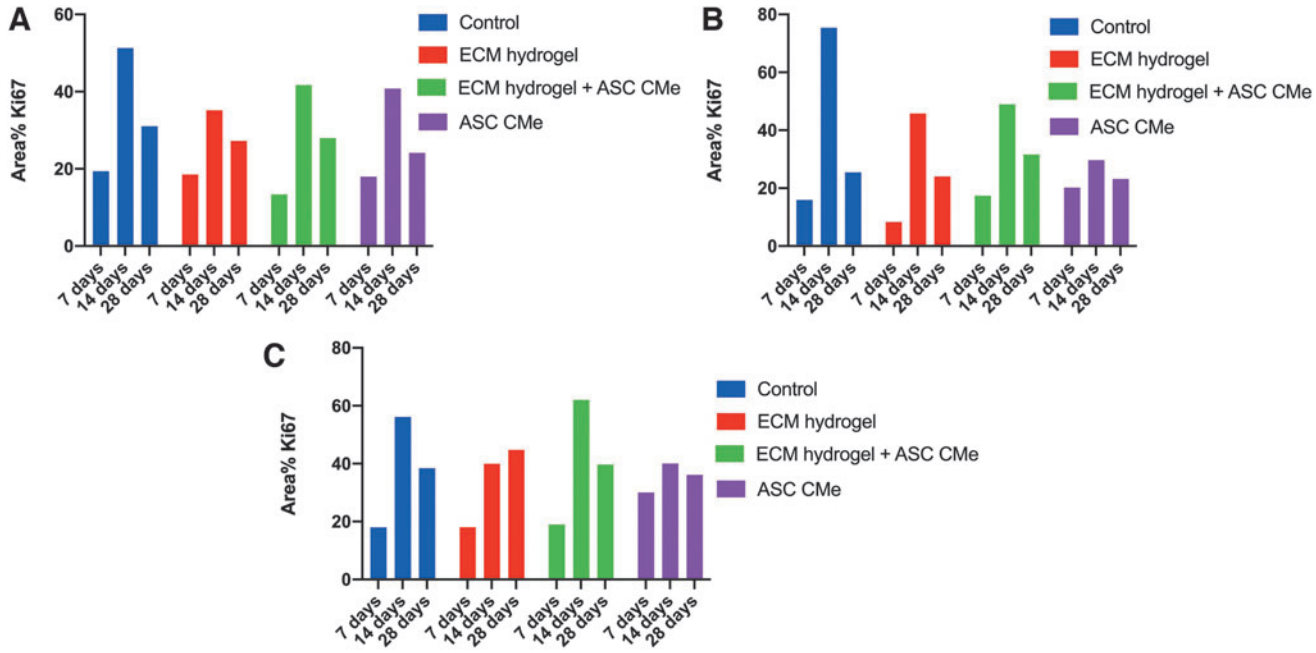

FIG. 6. Proliferation index in distal **(A)**, medial **(B),** and proximal **(C)** area based on Ki-67–positive cells in control, ECM hydrogel, ECM hydrogel + ASC-CMe, and ASC-CMe group after 7, 14, and 28 days ($n = 5$).

increase vascularity mainly in the most distal and ischemic part of the skin flap, but did not result in improved healing. Vascularity likely improved through ASCs' proangiogenic secretome and the stabilizing effect of ASCs, functioning as pericytes, on newly formed capillaries endothelial cells. ASCs' paracrine factors seem to induce a wound healing ''kick-start'' in heavily damaged tissue. In slightly damaged tissue, such as the middle and proximal part of the flap, it appears the innate immune response and wound healing capabilities are sufficient to heal tissue.

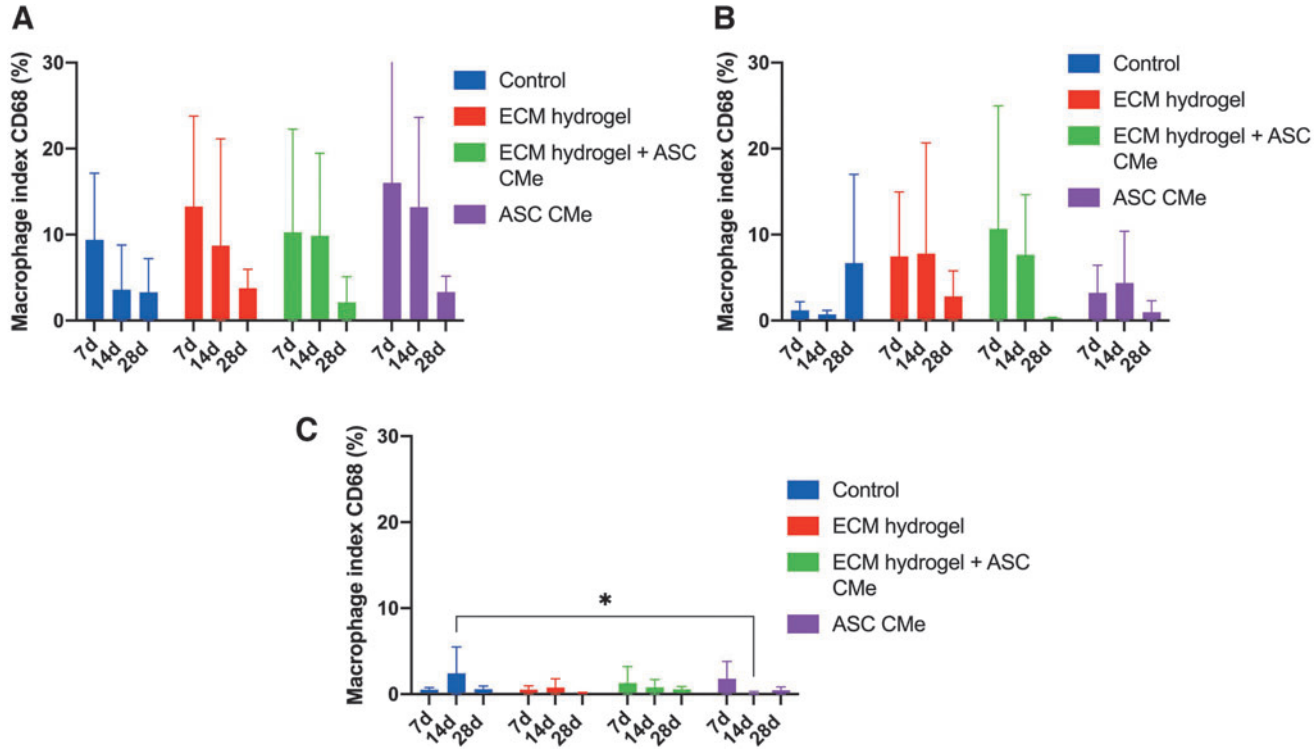

FIG. 7. Macrophage influx index in distal **(A)**, medial **(B),** and proximal **(C)** area based on CD68-positive cells in control, ECM hydrogel, ECM hydrogel + ASC-CMe, and ASC-CMe group after 7, 14, and 28 days ($n = 5$). Significantly lower CD68 expression in ASC-CMe group compared to the DMEM group after 14 days ($P < 0.05$*).

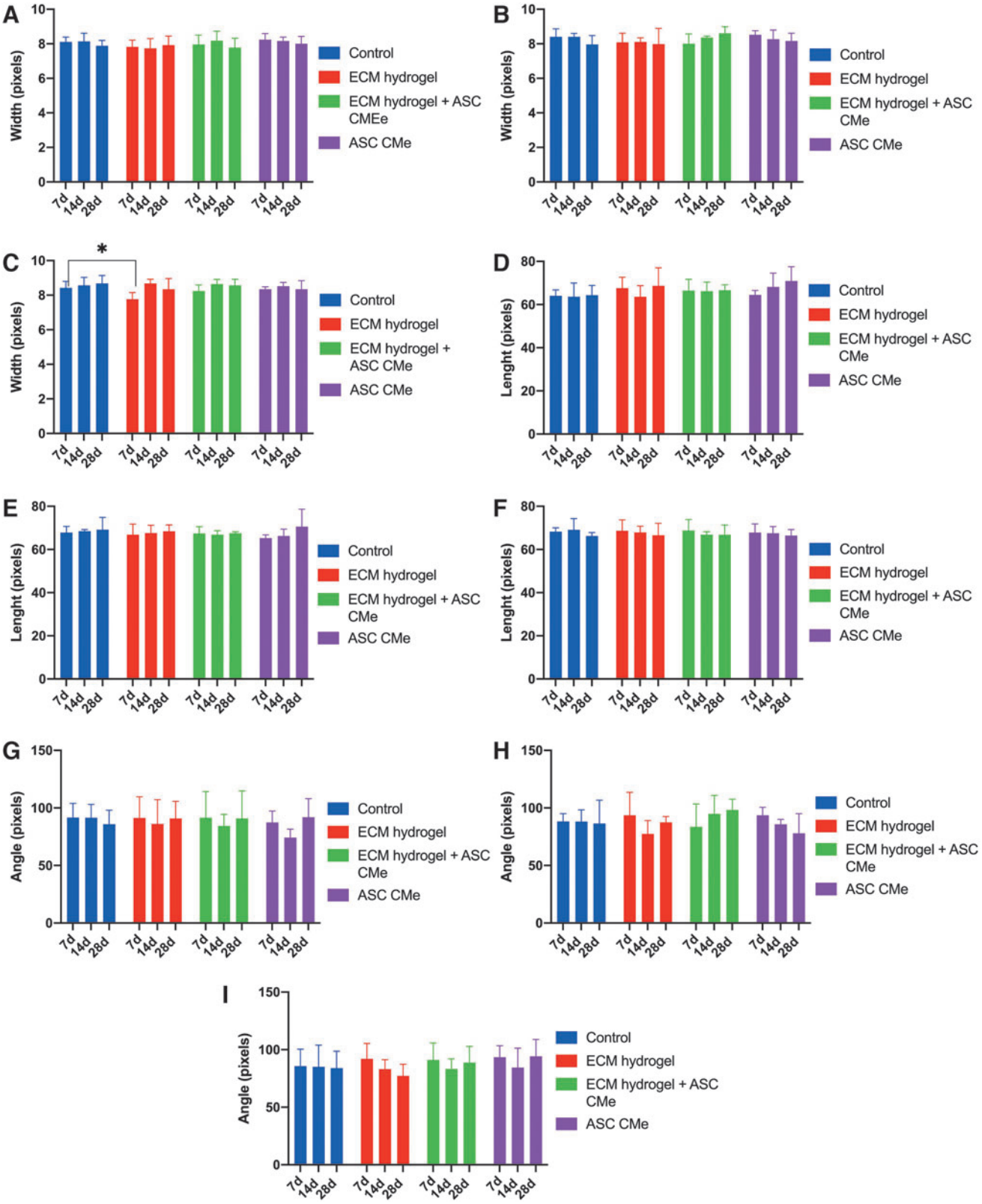

FIG. 8. Collagen remodeling in distal **(A, D, G)**, medial **(B, E, H)**, and proximal **(C, F, I)** area measured by collagen fiber width **(A–C)**, length **(D–F)**, and angle **(G–I)** in control, ECM hydrogel, ECM hydrogel + ASC-CMe, and ASC-CMe group after 7, 14, and 28 days ($n = 5$). Results were shown for distal **(A, D, G)**, medial **(B, E, H)**, and proximal **(C, F, I)** area of the wound. Significantly lower width in ECM hydrogel group compared with control group in the proximal area after 7 days ($P < 0.05$*).

The observed increased vascularity induced by ASC secretome is in accordance with findings of other studies [9,18–21,30]. Some of these studies concerned single growth factor administration, which has limitations, since only one agent in the wound healing process is stimulated to direct tissue regeneration. The single injection of vascular endothelial growth factor, for example, results in an increased formation of capillary tangle and unstable capillaries, which impairs the patency of blood flow. In addition, it is known that injected growth factors rapidly drain from damaged tissue when not sustained in a carrier. The therapeutical purpose of single growth factor administration seems therefore limited. Interestingly however, in this study ECM hydrogel with bound ASC secretome treatment did not increase vascularity as observed after ASC secretome treatment. This suggests that although the used concentration of secretome meets previous positive research results on angiogenesis, probably there are more important factors that are demanded to augment angiogenesis.

That the regenerative capability of ECM hydrogel with bound ASCs' secretome was not significantly reflected in this study's preclinical readouts, that is, improved wound healing, angiogenesis, increased proliferation, and altered ECM remodeling (aligned collagen fibers), may have several reasons or a combination. First, ASC secretome and ECM dosing in hydrogels influence therapeutic efficacy. ECM hydrogels bind and release secretome-based factors in a concentration-dependent manner.

It is feasible that lowly abundant factors in non- or 10-fold concentrated medium are released at rates and concentrations that are below biological efficacy. In fact, our previous research showed that hydrogels loaded with 100-fold concentration ASC secretome released high concentrations of angiogenic factors angiopoietins 1 and 2 and the chemoattractant CCL2 [10]. As for ECM dosing, a concentrated ECM hydrogel increases cytokine release, inducing inflammation, decreases trophic factor release, and influences hydrogels' viscoelastic properties, indirectly impacting cellular behavior.

However, no increased cytokine- or inflammatory status was observed. Viscoelastic properties have been investigated in vitro, but it could be interesting to investigate the effect of surrounding tissue on the viscoelastic properties of dECM hydrogels. Dosage also depends on the number of the applications of the treatment. Applying hydrogel treatment multiple times was considered but did not seem feasible because it would redamage the regenerated tissue below the skin flap.

Second, the retention of ECM hydrogel remains unclear. Microscopically, ECM hydrogel and native donor collagen fibers are indistinguishable in histological samples, which impairs determining if ECM hydrogel is still present and functional during follow-up. Moreover, the quantity and duration of growth factors' release could not be measured in this in vivo model. Nonetheless, Indian ink-doped ECM hydrogel was easily visible at the site of application after 24 h, indicating that it had solidified well and did not shift easily under the loose dorsal skin (Supplementary Movie). However, to precisely determine ECMs retention and growth factors' release profiles in vivo, a future study will employ fluorescently tagged ASC secretome or ECM hydrogel or both, to determine factor residence time or ECM hydrogel remnants.

Only few researchers have attempted to augment wound healing using this relatively new treatment modality. ECM hydrogel treatment in full thickness skin wounds in rodent resulted in increased angiogenesis, fastened re-epithelialization, and wound closure [31–35]. Additives were frequently used, for example, mesenchymal stem cells, endothelial cells, or growth factors. Although these models were mostly used to induce faster wound closure, the increased angiogenesis implies that ECM may definitely elicit positive effects on vascular perfusion, because increased vascularity was found irrespective of the abovenamed cells and additives. Thus, future research warrants fine-tuning of the manufacturing and (clinical) application of ECM hydrogels with bound ASC secretome to prove the possible regenerative effect.

Third, an important limitation of this study was the rather rapid wound healing of the controls, which may have obscured the beneficial influence of the treatments. Despite this disadvantage, the augmented angiogenesis in some treatment groups encourages to explore rats with defective wound healing (eg, in diabetic animals) or larger mammals such as pigs. The latter have a dermal wound healing more similar to human wound healing, yet are unsuitable to perform pilot studies such as the current one with rats. This study was limited to dermal wound healing in a pedicled skin flap. However, native tissue-based ECM hydrogels have been studied sufficiently in vitro to proceed to other preclinical purposes as well. The field is relatively new and still has high potential for future clinical applications.

Conclusion

In contrast to our expectations, we did not find evidence that ECM hydrogel loaded with ASC secretome leads to a faster dermal wound healing in a pedicled skin flap rat model as compared with control groups. ASC secretome however has shown proangiogenic potential.

Author Disclosure Statement

None of the authors had any conflict of interest in this study.

Funding Information

No funding was received for this article.

Supplementary Material

Supplementary Figure S1
Supplementary Figure S2
Supplementary Figure S3
Supplementary Figure S4
Supplementary Movie

References

1. Milton SH. (2005). Pedicled skin-flaps: the fallacy of the length: Width ratio*. Br J Surg 57:502–508.
2. Gümüş N, Y Odemiş, S Yılmaz and E Tuncer. (2012). Effect of topically applied minoxidil on the survival of rat dorsal skin flap. Aesthetic Plast Surg 36:1382–1386.
3. Hart K, D Baur, J Hodam, L Lesoon-Wood, M Parham, K Keith, R Vazquez, E Ager and J Pizarro. (2006). Short- and

long-term effects of sildenafil on skin flap survival in rats. Laryngoscope 116:522–528.
4. Davis RE, JH Wachholz, D Jassir, CA Perlyn and MH Agrama. (1999). Comparison of topical anti-ischemic agents in the salvage of failing random-pattern skin flaps in rats. Arch Facial Plast Surg 1:27–32.
5. Oh M, H Chang and KW Minn. (2008). The effects of tadalafil on axial-pattern skin flap survival in rats. Dermatol Surg 34:626–630; discussion 630.
6. Cai Y, Z Yu, Q Yu, H Zheng, Y Xu, M Deng, X Wang, L Zhang, W Zhang and W Li. (2019). Fat extract improves random pattern skin flap survival in a rat model. Aesthet Surg J 39:NP504–NP514.
7. Feng C-J, C-K Perng, C-H Lin, C-H Tsai, P-H Huang and H Ma. (2020). Intra-arterial injection of human adipose-derived stem cells improves viability of the random component of axial skin flaps in nude mice. J Plast Reconstr Aesthet Surg 73:598–607.
8. Spiekman M, JA van Dongen, JC Willemsen, DL Hoppe, B van der Lei and MC Harmsen. (2017). The power of fat and its adipose-derived stromal cells: emerging concepts for fibrotic scar treatment. J Tissue Eng Regen Med 11:3220–3235.
9. Foroglou P, V Karathanasis, E Demiri, G Koliakos and M Papadakis. (2016). Role of adipose-derived stromal cells in pedicle skin flap survival in experimental animal models. World J Stem Cells 8:101–105.
10. Liguori TTA, GR Liguori, JA van Dongen, LFP Moreira and MC Harmsen. (2020). Bioactive decellularized cardiac extracellular matrix-based hydrogel as a sustained-release platform for human adipose tissue-derived stromal cell-secreted factors. Biomed Mater 16:025022.
11. Zuk PA, M Zhu, P Ashjian, DA De Ugarte, JI Huang, H Mizuno, ZC Alfonso, JK Fraser, P Benhaim and MH Hedrick. (2002). Human adipose tissue is a source of multipotent stem cells. Mol Biol Cell 13:4279–4295.
12. Zuk PA, M Zhu, H Mizuno, J Huang, JW Futrell, AJ Katz, P Benhaim, HP Lorenz and MH Hedrick. (2001). Multilineage cells from human adipose tissue: implications for cell-based therapies. Tissue Eng 7:211–228.
13. Halvorsen YD, A Bond, A Sen, DM Franklin, YR Lea-Currie, D Sujkowski, PN Ellis, WO Wilkison and JM Gimble. (2001). Thiazolidinediones and glucocorticoids synergistically induce differentiation of human adipose tissue stromal cells: biochemical, cellular, and molecular analysis. Metabolism 50:407–413.
14. Halvorsen YD, D Franklin, AL Bond, DC Hitt, C Auchter, AL Boskey, EP Paschalis, WO Wilkison and JM Gimble. (2001). Extracellular matrix mineralization and osteoblast gene expression by human adipose tissue-derived stromal cells. Tissue Eng 7:729–741.
15. Erickson GR, JM Gimble, DM Franklin, HE Rice, H Awad and F Guilak. (2002). Chondrogenic potential of adipose tissue-derived stromal cells in vitro and in vivo. Biochem Biophys Res Commun 290:763–769.
16. Mizuno H, PA Zuk, M Zhu, HP Lorenz, P Benhaim and MH Hedrick. (2002). Myogenic differentiation by human processed lipoaspirate cells. Plast Reconstr Surg 109:199–209; discussion 210–211.
17. Lee W-CC, JP Rubin and KG Marra. (2006). Regulation of alpha-smooth muscle actin protein expression in adipose-derived stem cells. Cells Tissues Organs 183:80–86.
18. Khan A, H Ashrafpour, N Huang, PC Neligan, C Kontos, A Zhong, CR Forrest and CY Pang. (2004). Acute local subcutaneous VEGF165 injection for augmentation of skin flap viability: efficacy and mechanism. Am J Physiol Regul Integr Comp Physiol 287:R1219–R1229.
19. Ishiguro N, Y Yabe, T Shimizu, H Iwata and T Miura. (1994). Basic fibroblast growth factor has a beneficial effect on the viability of random skin flaps in rats. Ann Plast Surg 32:356–360.
20. Lineaweaver WC and F Zhang. (2014). Effects of CB-VEGF-A injection in rat flap models for improved survival. Plast Reconstr Surg 133:423e–424e.
21. Park HJ, S Lee, KH Kang, CY Heo, JH Kim, HS Yang and B-S Kim. (2013). Enhanced random skin flap survival by sustained delivery of fibroblast growth factor 2 in rats. ANZ J Surg 83:354–358.
22. van Dongen JA, V Getova, LA Brouwer, GR Liguori, PK Sharma, HP Stevens, B van der Lei and MC Harmsen. (2019). Adipose tissue-derived extracellular matrix hydrogels as a release platform for secreted paracrine factors. J Tissue Eng Regen Med 13:973–985.
23. Clause KC and TH Barker. (2013). Extracellular matrix signaling in morphogenesis and repair. Curr Opin Biotechnol 24:830–833.
24. Theocharis AD, SS Skandalis, C Gialeli and NK Karamanos. (2016). Extracellular matrix structure. Adv Drug Deliv Rev 97:4–27.
25. Martinez-Garcia FD, RHJ de Hilster, PK Sharma, T Borghuis, MN Hylkema, JK Burgess and MC Harmsen. (2021). Architecture and composition dictate viscoelastic properties of organ-derived extracellular matrix hydrogels. Polymers 13:3113.
26. Getova VE, JA van Dongen, LA Brouwer and MC Harmsen. (2019). Adipose tissue-derived ECM hydrogels and their use as 3D culture scaffold. Artif Cells Nanomed Biotechnol 47:1693–1701.
27. Liguori GR, TTA Liguori, SR de Moraes, V Sinkunas, V Terlizzi, JA van Dongen, PK Sharma, LFP Moreira and MC Harmsen. (2020). Molecular and biomechanical clues from cardiac tissue decellularized extracellular matrix drive stromal cell plasticity. Front Bioeng Biotechnol 8:520.
28. Camargo CP, NF Margarido, E Guandelini, GAB Vieira, AL Jacomo and R Gemperli. (2014). Description of a new experimental model skin flap for studying skin viability in rats. Acta Cir Bras 29:166–170.
29. Crapo PM, TW Gilbert and SF Badylak. (2011). An overview of tissue and whole organ decellularization processes. Biomaterials 32:3233–3243.
30. Zhang P, J Feng, Y Liao, J Cai, T Zhou, M Sun, J Gao and K Gao. (2018). Ischemic flap survival improvement by composition-selective fat grafting with novel adipose tissue derived product - stromal vascular fraction gel. Biochem Biophys Res Commun 495:2249–2256.
31. Lee C, S Shim, H Jang, H Myung, J Lee, C-H Bae, JK Myung, M-J Kim, SB Lee, et al. (2017). Human umbilical cord blood–derived mesenchymal stromal cells and small intestinal submucosa hydrogel composite promotes combined radiation-wound healing of mice. Cytotherapy 19:1048–1059.
32. Morris AH, H Lee, H Xing, DK Stamer, M Tan and TR Kyriakides. (2018). Tunable hydrogels derived from genetically engineered extracellular matrix accelerate

diabetic wound healing. ACS Appl Mater Interfaces 10: 41892–41901.
33. Savitri C, SS Ha, E Liao, P Du and K Park. (2020). Extracellular matrices derived from different cell sources and their effect on macrophage behavior and wound healing. J Mater Chem B 8:9744–9755.
34. Ha SS, ES Song, P Du, M Suhaeri, JH Lee and K Park. (2020). Novel ECM patch combines Poly(vinyl alcohol), human fibroblast-derived matrix, and mesenchymal stem cells for advanced wound healing. ACS Biomater Sci Eng 6:4266–4275.
35. Du P, M Suhaeri, SS Ha, SJ Oh, S-H Kim and K Park. (2017). Human lung fibroblast-derived matrix facilitates vascular morphogenesis in 3D environment and enhances skin wound healing. Acta Biomater 54:333–344.

Address correspondence to:
Martin C. Harmsen, PhD
Department of Pathology and Medical Biology
University Medical Center Groningen
University of Groningen
Hanzeplein 1-EA11
Groningen 9713 GZ
the Netherlands

E-mail: m.c.harmsen@umcg.nl

Received for publication January 8, 2022
Accepted after revision May 17, 2022
Prepublished on Liebert Instant Online May 18, 2022